J Biomol NMR (2015) 62:71–79
DOI 10.1007/s10858-015-9920-0

ARTICLE

Antimicrobial peptide protegrin-3 adopt an antiparallel dimer in the presence of DPC micelles: a high-resolution NMR study

K. S. Usachev[1,2] · S. V. Efimov[1] · O. A. Kolosova[1] · E. A. Klochkova[1] · A. V. Aganov[1] · V. V. Klochkov[1]

Received: 12 February 2015 / Accepted: 14 March 2015 / Published online: 19 March 2015

Abstract A tendency to dimerize in the presence of lipids was found for the protegrin. The dimer formation by the protegrin-1 (PG-1) is the first step for further oligomeric membrane pore formation. Generally there are two distinct model of PG-1 dimerization in either a parallel or antiparallel β-sheet. But despite the wealth of data available today, protegrin dimer structure and pore formation is still not completely understood. In order to investigate a more detailed dimerization process of PG-1 and if it will be the same for another type of protegrins, in this work we used a high-resolution NMR spectroscopy for structure determination of protegrin-3 (RGGGL-CYCRR-RFCVC-VGR) in the presence of perdeuterated DPC micelles and demonstrate that PG-3 forms an antiparallel NCCN dimer with a possible association of these dimers. This structural study complements previously published solution, solid state and computational studies of PG-1 in various environments and validate the potential of mean force simulations of PG-1 dimers and association of dimers to form octameric or decameric β-barrels.

Keywords NMR · Structure · Protegrin · Dimer · Antimicrobial peptide · DPC micelle

Introduction

Protegrins are a potent antimicrobial, β-hairpin, cationic peptides isolated from porcine leukocytes (Fahrner et al. 1996; Jenssen et al. 2006; Kokryakov et al. 1993). These small β -sheet antimicrobial peptides (AMPs) are members of the cathelicidin family (Zhao et al. 1994, 1995), a large group of structurally diverse AMPs whose precursors contain a highly conserved cathelin domain (Zanetti et al. 1995). Naturally occurring AMPs probably represent one of the very first evolved forms of chemical defense of living eukaryotic cells against invasion by bacteria, protozoa, fungi, and virus. AMPs are less susceptible to the development of bacterial resistance because they disrupt the membrane of bacteria through non-specific peptide–lipid interactions. The urgent need for new antibiotics has stimulated interest in the development of AMPs as human therapeutics and amplified interest in the development of biophysical approaches to probe their mechanism (Ramamoorthy 2009). Natural AMPs have such properties as the broad spectrum antibacterial activity, high selectivity, and the disruption of bacterial cell membranes, what allow to suggest that these molecules are potentially useful as antibiotics; so it is important to investigate their structure and function at high resolution in order to increase their potency and selectivity (Porcelli et al. 2008; Ramamoorthy 2009). Therefore, high-resolution structures of these peptides in a suitable membrane environment and characterization of the

Database Structural data are available in the Protein Data Bank/BioMagResBank databases under the accession numbers 2MZ6/25474.

Electronic supplementary material The online version of this article (doi:10.1007/s10858-015-9920-0) contains supplementary material, which is available to authorized users.

✉ K. S. Usachev
k.usachev@kpfu.ru

[1] NMR Laboratory, Institute of Physics, Kazan Federal University, Kremlevskaya, 18, Kazan 420008, Russian Federation

[2] Laboratory of Structural Biology, Institute of Fundamental Medicine and Biology, Kazan Federal University, Kremlevskaya, 18, Kazan 420008, Russian Federation

oligomerization of membrane-associated peptides are important to understand the folding and function of biomolecules like AMPs, fusion peptides, amyloid peptides, toxins, and ion channels (Ramamoorthy et al. 2008). Despite the wealth experimental approaches available today such as X-ray diffraction, solid state NMR and high-resolution solution NMR studies, the amphipathic properties of the cell membrane components are not suitable for most biophysical techniques. Particularly, lipids and membrane-associated peptides and proteins are difficult to solubilize in water for high-resolution solution NMR studies and difficult to crystallize for X-ray diffraction studies. Therefore, there is a significant need for the development of new high-resolution techniques to probe lipid-peptide and peptide–peptide interactions that lead to the oligomerization process (Porcelli et al. 2008; Ramamoorthy et al. 2008). Previously several NMR structural studies of oligomeric forms of such AMPs as MSI-78 (Ramamoorthy et al. 2008), LL-37 (Porcelli et al. 2008) and PG-1 (Mani et al. 2006) have been reported.

In order to understand mechanisms of action, atomic-resolution structures of oligomeric forms of AMPs in lipid environments (either in micelles or in bilayers), are highly necessary (Saravanan and Bhattacharjya 2011). The oligomerization of AMPs on contact with their target membranes is known to be crucial to their biological action (Gottler et al. 2008; Epand et al. 2006; Papo and Shai 2004). But despite that lipid bilayers are closer mimic to the native cellular membranes, the atomic resolution structures of AMPs in such systems are difficult to obtain due to the large sizes (Haney et al. 2009; Ramamoorthy 2009). Recently several solid state NMR studies have been reported a successful determination of oligomerization and structural studies of AMPs in lipid bilayer (Hong 2006; Ramamoorthy et al. 2008; Afonin et al. 2011). And on the other hand, atomistic resolution structures, by use of solution NMR techniques, of AMPs are mostly determined in the context of small and fast tumbling detergent micelles [Sodium dodecyl sulfate (SDS), dodecylphosphocholine (DPC) or dioctanoyl phosphatidylglycerol (D8PG) micelles] (Chan et al. 2006; Powers et al. 2005; Wang 2007). Although in a large number of studies suggest that these lipid micelles predominantly favor monomeric structures of AMPs, oligomerization or dimerization for some AMPs also have been detected in DPC micelles e.g. helical dimers of magainin analog MSI-78 (Porcelli et al. 2008), protegrin-1 (Roumestand et al. 1998), arenicins (Ovchinnikova et al. 2008) and pleurocidin (Syvitski et al. 2005). DPC micelles also are more frequently used, as compared to SDS micelles, as a model membrane mimic for structural studies of membrane proteins (Hiller and Wagner 2009; Arora and Tamm 2001; Zamoon et al. 2005).

Protegrins (PG-1–PG-5) are antibacterial peptides of 16–18 residues whose structure has been shown to be a β-hairpin stabilized by two disulfide bonds (Fahrner et al. 1996). The most studied of these is the protegrin-1 (PG1) which is composed of 18 amino acids residues (PDB ID: 1PG1, 1ZY6) and supposed that PG-1 forms ion channels in membranes and kills bacteria involves oligomeric peptide toroidal pores in anionic lipid bilayer membranes, which mimic the inner membrane of Gram-negative bacteria (Langham et al. 2008; Mani et al. 2006). Also have been developed several synthetic mimetics of protegrins, there linear analogs and one variant named IB-367 or Iseganan HCl has been considered for the treatment of various conditions over the last 15 years, but a drug has not yet been approved. (Elad et al. 2012; Lazaridis et al. 2013; Loury et al. 1999; Trotti et al. 2004).

Several experimental and computational structural studies of PG in monomer and oligomer forms were reported (Buffy et al. 2003; Fahrner et al. 1996; Jang et al. 2006, 2007; Lazaridis et al. 2013; Mani et al. 2006; Roumestand et al. 1998; Usachev et al. 2014a; Vivcharuk and Kaznessis 2010; Yamaguchi et al. 2002). Protegrin monomers interact very weakly with the surface of the zwitterionic membranes, but adsorb readily on the surface of anionic membranes (Lazaridis et al. 2013). It was found that the protegrin has a tendency to dimerize in the presence of lipids. The dimer formation by the PG-1 is the first step for further oligomeric membrane pore formation, since the dimer can be regarded as the primary unit for assembly into the ordered aggregates (Jang et al. 2007).

Generally there are two distinct model of PG-1 dimerization in either a parallel (have been observed on the surface of cholesterol-containing zwitterionic lipid bilayers) or antiparallel β-sheet orientation (observed on the surface of DPC micelles) (Mani et al. 2006; Roumestand et al. 1998). The structure of a parallel PG-1 dimer has been determined by solid-state NMR and deposited with PDB code 1ZY6, but currently there is no atomistic resolution structure of the antiparallel dimer structure. Although solid-state NMR revealed a parallel NCCN orientation is dominant in water, in the transmembrane inserted state was found that a parallel NCCN dimerization is not favorable for interaction with either flat membranes or pores (Lazaridis et al. 2013). The results of molecular dynamics simulations to calculate potential of mean force (PMF) are consistent with the results of NMR experimental observations which determined that the PG-1 dimer adopts an antiparallel structure upon binding to DPC micelles (Roumestand et al. 1998; Vivcharuk and Kaznessis 2010). The different alignment likely results from the significant curvature difference between the small-radius micelles and the flatter and more biological lipid bilayers. The different packing motifs of PG-1 between the lipid bilayer and the micelle underscore the importance of the environment for the oligomerization of membrane peptides

and the plasticity of the PG-1 structure (Mani et al. 2006). Nevertheless despite the wealth of data available today, protegrin pore formation is still not completely understood.

However, even for PG-1 there are a lot of experimental and theoretical studies, for another protegrins (PG-2, PG-3, PG-4, PG-5) structural studies are almost have not been investigated and biological functions among the different protegrins is also still limited (Choi et al. 2014; Kokryakov et al. 1993; Zhao et al. 1994, 1995). Amino acid sequences of these five protegrins are almost identical, except for 1–3 amino acid substitutions. Cho et al. (1998) found that both PG-1 and enantiomeric PG-1 (composed exclusively of D-amino acids) were potently fungicidal for yeast-phase *Candida albicans*. The protegrins PG-2, -3, and -5, but not PG-4, were as effective as PG-1. These studies suggest that only 12 residues are needed to endow protegrin molecules with strong antibacterial activity and that at least 4 additional residues are needed to add potent antifungal properties. Thus, the 16-residue protegrin PG-2 likely represents the minimal structure needed for broad-spectrum antimicrobial activity encompassing bacteria and fungi. In order to investigate a more detailed dimerization process of PG-1 and if it will be the same for another type of protegrins, in this work we used a high-resolution NMR spectroscopy for structure determination of protegrin-3 (RGGGL-CYCRR-RFCVC-VGR) in the presence of perdeuterated DPC micelles (Roumestand et al. 1998). This protegrin substitutes a glycine for an arginine at position 4 and it has one less positive charge than PG-1.

Materials and methods

Sample preparation

PG-3 peptide was synthesized by Dr. Andrey Filippov in Chemistry of Interfaces laboratory at the Luleå University of Technology as previously described (Usachev et al. 2014a). The purity of the peptide was estimated as better than 95 %. The sample was lyophilized and stored at a temperature of 193 K before use.

The NMR samples of PG-3 were prepared as previously described for PG-1 in DPC micelles (Roumestand et al. 1998). The peptide (4 mg) was solubilized in an aqueous solution at pH 3.5 (H_2O or ^2H_2O, 500 µl) containing 20 mg perdeuterated DPC (molar ratio ~1:12). 3-(trimethylsilyl)-propionic-2,2,3,3-$^2H_4$ acid (TMSP-2,2,3,3-$^2H_4$) (98 % atom ^2H, Aldrich) was added as an internal chemical shift standard for ^1H NMR spectroscopy. Perdeuterated d_{38} DPC (98 % ^2H) and TSP-d_4 were purchased from Aldrich.

NMR spectroscopy and spatial structure calculation

All data were acquired at 700 MHz (Bruker Avance III HD) NMR spectrometer equipped with quadruple resonance (^1H, ^{13}C, ^{15}N and ^{31}P) CryoProbe. The sample temperature was set to temperature 293 K. The proton chemical shifts were referred to the TMSP-2,2,3,3-$^2H_4$.

Two-dimensional (2D) experiments (DQF-COSY, TOCSY, and NOESY) spectra were acquired in the phase-sensitive mode using the States-TPPI method and using a time domain data size of 512 t_1 × 4096 t_2 complex points and 32 transients per complex t_1 increments. The water resonance was suppressed by "3-9-19" pulse sequence with gradients using flip-back pulse in COSY experiments (Piotto et al. 1992; Sklenar et al. 1993) and using excitation sculpting with gradients in TOCSY and NOESY experiments (Hwang and Shaka 1995). TOCSY spectra were obtained with a mixing time of 80 ms and NOESY spectra with a mixing time of 200 ms.

2D ^1H-^{13}C HSQC, ^1H-^{13}C HSQC-TOCSY, ^1H-^{13}C HMBC and ^1H-^{15}N HSQC spectra were recorded with 512 (^1H) × 4096 (^{13}C and ^{15}N) complex points, respectively, for spectral widths of 13 (^1H), 35 (^{15}N), and 200 ppm (^{13}C). The ^1H, ^{13}C, and ^{15}N chemical shifts of PG-3 are available in the BioMagResBank (BMRB ID 25474).

Spectra were processed by NMRPipe (Delaglio et al. 1995) and analyzed using SPARKY. Sequence-specific backbone resonance assignments and side-chain assignments for all residues were obtained using a combination of 2D COSY, TOCSY and NOESY experiments for ^1H signals, by 2D ^1H-^{13}C HSQC, ^1H-^{13}C HSQC-TOCSY, ^1H-^{13}C HMBC for ^{13}C signals and by ^1H-^{15}N HSQC for ^{15}N.

Inter-proton distances obtained from analysis of intensities of cross-peaks from NMR NOESY spectra were used as the primary data for the calculations by the molecular dynamics method. Following structural calculations, the ensemble of structures was subjected to restrained molecular dynamics using the Xplor-NIH (Schwieters et al. 2003). A total of 1000 structures were calculated and 20 with minimal energy were chosen. None of the 20 structures had any violated nuclear Overhauser effect (NOE) distances. Individual structures were minimized, heated to 1000 K for 6000 steps, cooled in 100 K increments to 50 K, each with 3000 steps, and finally minimized with 1000 steps of the steepest descent, followed by 1000 steps of conjugate gradient minimization. Starting with a family of 1000 structures, approximately 200 were subjected to subsequent molecular dynamics calculations and, finally, the 20 lowest energy structures were retained. To calculate the 3D structures of the PG-3 dimer the same protocol was used where the distance restraints were used as input in the standard distance geometry (DG)/simulated annealing (SA) refinement and energy minimization protocol (Schwieters

et al. 2003). The program MolProbity (Chen et al. 2010; Davis et al. 2007) was used to assess the overall quality of the structures. The PG-3 peptide structures were visualized with CHIMERA (Pettersen et al. 2004).

Results and discussion

Proton chemical shift assignments of PG-3 in DPC micelles were obtained using standard methods of protein NMR spectroscopy by 2D NMR ^{1}H–^{1}H TOCSY and NOESY experiments; by 2D ^{1}H–^{13}C HSQC, HSQC-TOCSY and HMBC experiments for carbon and by ^{1}H–^{15}N HSQC experiment for nitrogen nuclei (Table 1). Due to natural abundance of the ^{13}C and ^{15}N nuclei in peptide only ~72 % of ^{13}C and ^{15}N signals were assigned. Chemical shifts were deposited in the BioMagResBank (BMRB ID 25474).

Figure 1 shows the fingerprint region of the ^{1}H-^{1}H COSY, ^{1}H-^{1}H NOESY, ^{1}H-^{13}C and ^{1}H-^{15}N HSQC spectra of PG-3 at 293 K in H_2O solution and in the presence of DPC at a detergent/protein ratio of ~12. The presence of numerous well-resolved cross-peaks in the NOESY spectra along with the significant degree of spectral dispersion in the amide region and the presence of $dNN_{(i,i+1)}$ and $d\alpha N_{(i,i+1)}$ medium range NOE connectivities (Fig. 2) in 2D NOESY NMR spectra of PG-3 in DPC micelles is a strong indication that the peptide is at least partially folded, as a completely disordered structure would have both poor chemical shift dispersion due to the similarity of chemical shift values in the random coil state and poor NOE cross-peak intensity due to the high mobility of the structure (Khayrutdinov et al. 2009; Kim et al. 2011; Usachev et al. 2013, 2014b).

Two disulfide bonds (Cys6-Cys13 and Cys8-Cys15) and summary of the sequential and medium-range NOEs allow us to suggest that the PG-3 adopts a β-hairpin in the presence of DPC. Similarly, the nine amide protons potentially involved in H-bonds in the β-sheet were found as slowly exchanging protons, whereas they were exchanging in less than 5 min in D_2O solution (indicated with a filled circle in Fig. 2). Exchange rates between water and H_N protons were analysed by detection of peaks in ^{1}H and ^{1}H–^{1}H TOCSY spectra and observed cross-peaks were treated as an indication of water-exposed amide groups. In NOESY NMR spectra of PG-3 besides the β-sheet regular NOEs we also observed some additional NOEs between sidechains which appear inconsistent with the β-sheet structure (see Figure 1S and Table 1S). For example there were 8 NOE effects observed between residues F12 and F16, V14 and C15, V14 and V16, C15 and V16 which are far apart in the β-sheet structure. We assume that these

Table 1 ^{1}H, ^{13}C and ^{15}N chemical shifts in ppm measured in water for PG-3 in the presence of predeuterated DPC micelles (detergent/peptide molar ratio ~12) at 293 K

Residue	Chemical shift (ppm)											
	NH	$C_\alpha H$	$C_\beta H$	$C_\gamma H$	$C_\delta H$	$C_\varepsilon H$	N	N_ε	C_α	C_β	C_γ	C_δ
R1	–	4.03	1.87	1.62, 1.53	3.14	7.35	–	–	52.99	28.05	23.56	40.52
G2	8.94	4.02	–	–	–	–	111.6	–	42.61	–	–	–
G3	8.48	3.94	–	–	–	–	109.0	–	42.73	–	–	–
G4	8.82	3.87	–	–	–	–	110.4	–	43.71	–	–	–
L5	8.66	4.13	1.67	1.54	0.88, 0.83	–	122.9	–	54.44	39.03	24.46	22.41, 21.43
C6	8.31	4.64	2.87	–	–	–	118.7	–	58.78	24.37	–	–
Y7	8.01	4.23	3.07	–	7.05	6.71	120.1	–	57.82	40.69	–	130.6
C8	8.10	4.03	3.01, 2.69	–	–	–	117.5	–	52.87	24.84	–	–
R9	8.33	3.94	1.92, 1.76	1.59	3.10	7.49	120.0	–	56.41	27.47	24.68	40.67
R10	7.90	4.04	1.76	1.61, 1.52	3.09	7.21	–	84.83	55.60	27.48	23.64	40.53
R11	7.96	3.99	1.76	1.53, 1.25	2.97, 2.87	7.40	117.4	–	54.35	27.48	24.05	39.94
F12	8.14	4.35	3.19, 2.98	–	7.05	7.14	–	–	56.97	36.98	–	126.6
C13	8.05	4.16	2.96, 2.89	–	–	–	119.9	–	58.49	24.43	–	–
V14	7.84	3.93	2.06	0.92, 0.87	–	–	–	–	61.05	29.86	18.77	–
C15	8.05	4.28	2.85, 2.81	–	–	–	117.2	–	57.86	25.19	–	–
V16	7.74	4.08	2.03	0.72	–	–	–	–	59.49	29.63	–	–
G17	8.00	3.86	–	–	–	–	110.4	–	42.78	–	–	–
R18	7.87	4.24	1.85	1.60, 1.53	3.10	7.35	121.9	–	53.06	28.54	24.66	40.64

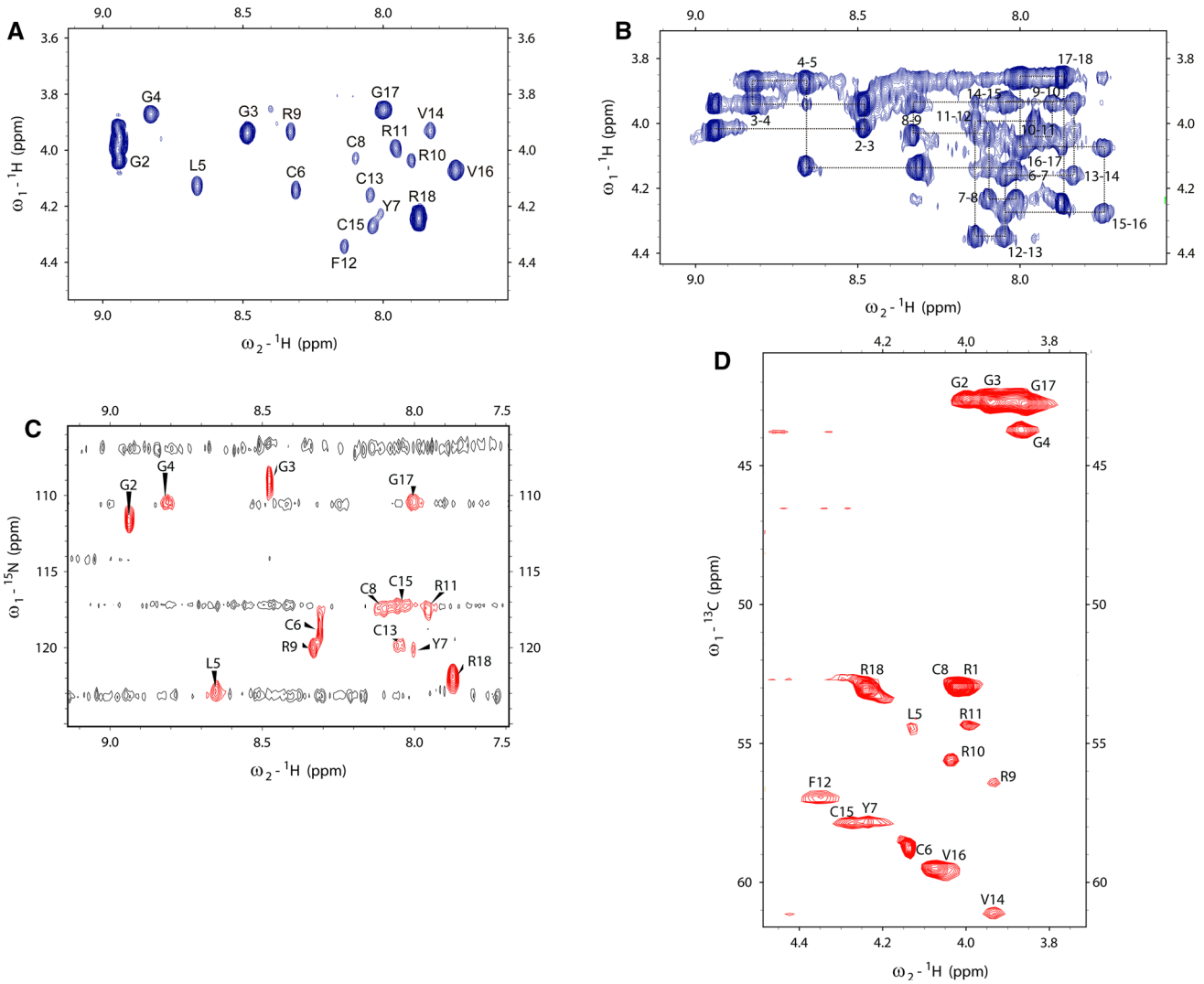

Fig. 1 Fingerprint regions of 2D NMR spectra (**a** ^{1}H–^{1}H COSY; **b** ^{1}H–^{1}H NOESY; **c** ^{1}H–^{15}N HSQC; **d** ^{1}H–^{13}C HSQC) acquired at 700 MHz with cryoprobe of PG-3 in a solution of $H_2O + D_2O$ with DPC micelles

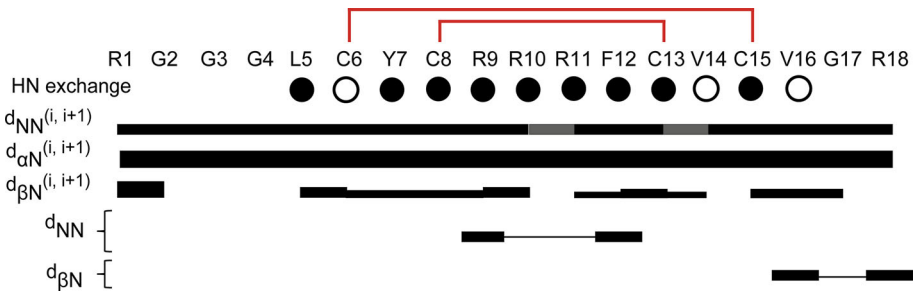

Fig. 2 Summary of the sequential and medium-range NOEs for the PG-3 in a solution of $H_2O + D_2O$ with DPC micelles. The relative intensity of NOEs is represented by the thickness of the *bars*. When an unambiguous assignment was not possible due to peak overlap, the NOEs are drawn with *gray shaded boxes*. Slowly and intermediate-exchanging protons are identified by *filled and empty circles*, respectively. The two disulfide bonds are displayed in *red*

NOE are not intramolecular but intermolecular effects and that two monomers of protegrin-3 adopt an antiparallel NCCN β-sheet (Roumestand et al. 1998).

A total of 167 interproton NOE distance constraints were determined for the structural calculations of PG-3 (see Table 2). At the first stage the 3D structure of PG-3 monomer in the presence of DPC micelles was constructed by molecular dynamics method calculations of the Xplor-NIH program (Schwieters et al. 2003). The 20 lowest-energy structures of PG-3 were used for the final analysis. Then the obtained monomer structure was used for further PG-3 dimer 3D structure calculation by the protocol where the distance restraints were used as input in the standard DG/SA refinement and energy minimization protocol (Schwieters et al. 2003). The final low-energy dimer that agrees with all of the intermolecular distance constraints have been deposited in the Protein Data Bank with the code 2MZ6. Superimposed conformations of the minimized structures for the PG-3 in a solution of $H_2O + D_2O$ with DPC micelles are shown in Fig. 3. Most of the structure is well defined with a an overall backbone root mean squared deviation of 1.37 Å. As expected from the NOE crosspeak patterns, PG-3 adopted an anti-parallel NCCN β sheet from residues 4–9 and 12–17 (Fig. 4). The overall quality of the structures was assess by the program MolProbity (Chen et al. 2010; Davis et al. 2007). 77.8 % for monomer and 93.8 % for dimer of all residues were in favored (98 %) regions and 100.0 % of all residues were in allowed (>99.8 %) regions. None of the 20 structures had any violated NOE distances.

Despite the NOE effects observed between residues F12 and F16, V14 and C15, V14 and V16, C15 and V16 which were explained by the formation of an additional antiparallel β-sheet between the two monomers, there were several signals in NOESY spectra between residues L5 and C8 (L5 $C_\alpha H$ and C8 $C_\beta H$; L5 $C_\alpha H$ and C8 HN; L5 $C_\delta H$ and C8 $C_\beta H$) (see Figure 1S and Table 1S). More over the slow exchange exhibited by the amide protons of residues C6 and C8 suggests a possible dimers association because these residues are located on the outer strands of the large four-stranded β-sheet formed by the dimer, and their corresponding NH protons are not involved in the regular

Table 2 Structural statistics for the NMR structure of dimer PG-3 in a solution of $H_2O + D_2O$ with DPC micelles

Distance restraints used for structure calculation	Total
Intraresidue ($\|i - j\| = 0$)	54
Sequential ($\|i - j\| = 1$)	90
Medium-range ($1 < \|i - j\| \leq 4$)	11
Long-range ($\|i - j\| > 4$)	0
Total intermonomer contacts	155
Total intramonomer contacts	12

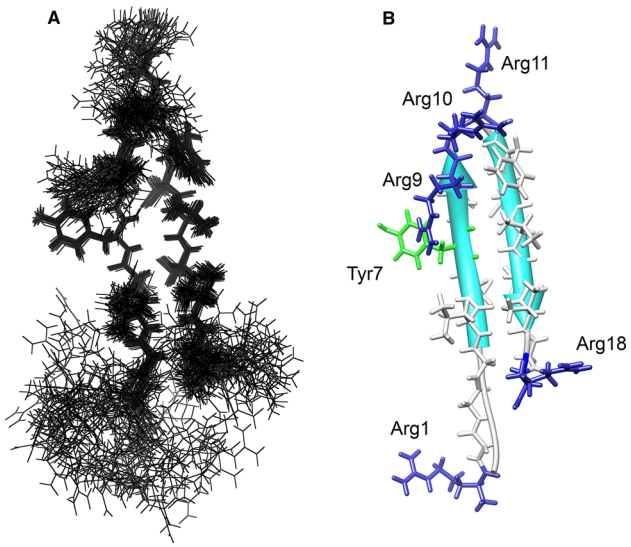

Fig. 3 Superimposed conformations of the 50 minimized structures for the PG-3 in a solution of $H_2O + D_2O$ with DPC micelles. **a** Only backbone atoms shown as *sticks*; **b** the backbone is shown in *ribbon* representation, the side-chains in *stick* representation, hydrophobic residues and disulfide-bonded Cys residues are shown in *white*, a polar residue (Tyr) are shown in green, and positively charged residues (Arg) are shown in *blue*

H-bond pattern of the dimer. Based on the data mentioned above we could assume that these NOEs might stabilize further association of protegrin-3 dimer. This is consistent with such models like the octamer formation in membrane pores (Lazaridis et al. 2013) and "carpeting" model (Shai 2002) that describes the initial association of AMPs with the membrane surface prior to membrane disruption; essentially the membrane surface is saturated with peptide. Such inter-dimer NOEs were expected but not observed previously for PG-1 dimer, so our data complements previously published solution structure of PG-1 dimer and validates the antiparallel NCCN model (Roumestand et al. 1998). Two valine residues, at positions 14 and 16, together with Phe12 form a hydrophobic cluster that contributes to the amphipathic character of the peptide (Gottler et al. 2008). Likewise in our dimer structure of PG-3 the hydrophobic cluster and SS bonds line are oriented in opposite directions. Due to that fact that a membrane surface with positive curvature allows the hydrophobic cluster to be buried while the charged residues remain solvated in water here we speculate that hydrophobic cluster residues are oriented toward the micelle (Galiullina et al. 2012; Blochin et al. 2013) and the SS bonds line oriented in opposite direction inside the toroidal pore, as shown by explicit simulations in previous works (Jang et al. 2008; Langham et al. 2008; Lazaridis et al. 2013). Proposed conformation of protegrin-3 octamer in membrane pores is present in Fig. 5. Generally our data are in a good

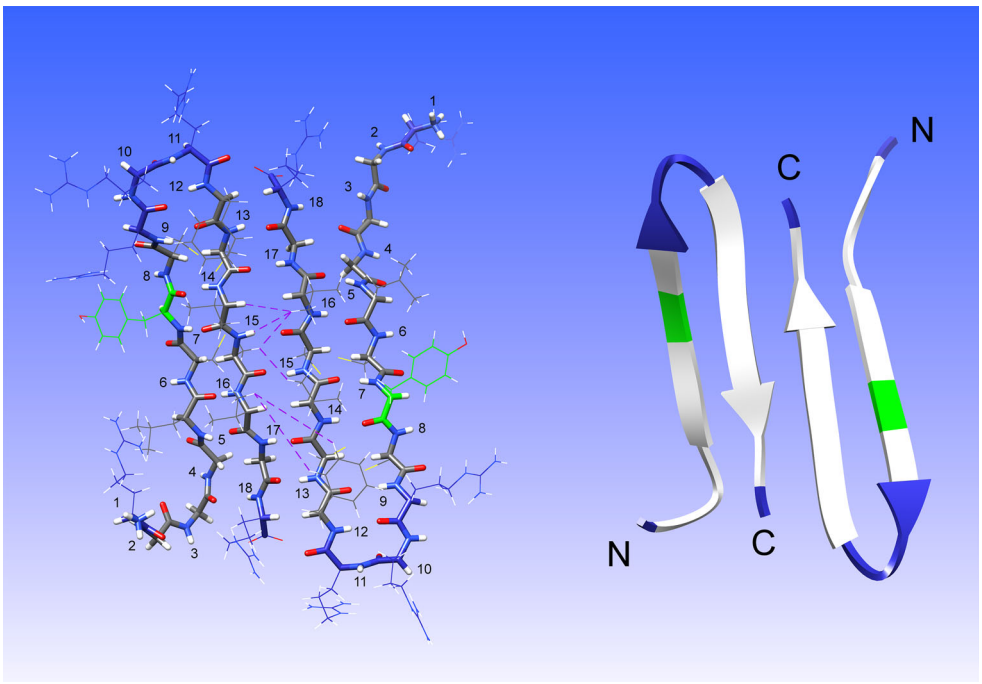

Fig. 4 Cartoon of PG-3 dimer (2MZ6) in stereo view, representing the NMR structure. Hydrophobic residues and disulfide-bonded Cys residues are shown in *white*, a polar residue (Tyr) are shown in *green*, and positively charged residues (Arg) are shown in *blue*. The intermonomer NOEs (dimer contacts) are shown as *magneta dotted lines*

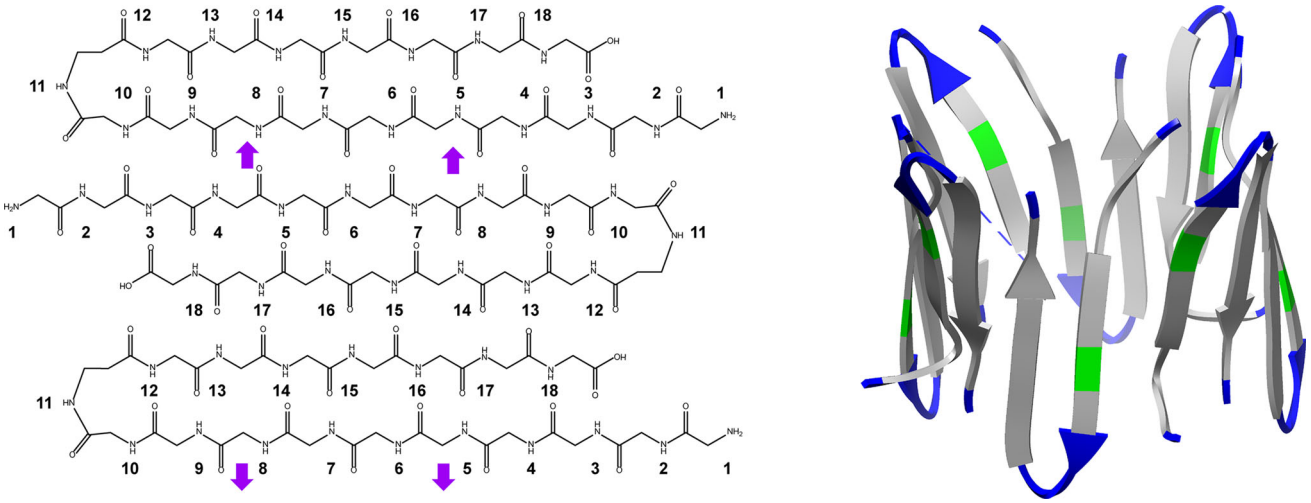

Fig. 5 The secondary structure of PG-3 in the presence of DPC micelles. The filled arrows indicate intermolecular NOEs efects which might stabilize further association. In the cartoon hypotitazes conformation of protegrin-3 octamer in membrane pores is present. Hydrophobic residues and disulfide-bonded Cys residues are shown in *white*, a polar residue (Tyr) are shown in *green*, and positively charged residues (Arg) are shown in *blue*

agreement with PMF calculation which shown that the antiparallel NCCN octamers are stable and exhibit a favorable binding energy to the pore (Lazaridis et al. 2013).

Conclusion

In this article, we report the monomer and dimer (2MZ6) conformation of the PG-3 in the presence of DPC micelles studied by 2D NMR spectroscopy. Our results demonstrate that PG-3 forms an antiparallel NCCN dimer in the presence of DPC micelles, and suggest that there is a possible association of these dimers which corresponded with the evidence for the existence of the antiparallel state of a PG-1 dimer on the surface of the membrane. This structural study allow to validate the antiparallel NCCN model for PG-1 and complements previously published solution NMR study of PG-1 in DPC micelles (Roumestand et al. 1998) and PMF simulations (Vivcharuk and Kaznessis 2010) which found that the peptide forms antiparallel

NCCN dimers and association of dimers to form octameric or decameric β-barrels.

We believe our results, presented in this paper, provide a foundation for further studies of protegrins PG-1-PG-5 structure, the mechanism of pores formation and a rationalization for the peptide's cytotoxicity.

Acknowledgments We thank Dr. Andrey Filippov for peptide synthesized. The work is performed accordingly to the Russian Government Program of Competitive Growth of Kazan Federal University; by the subsidy allocated to Kazan Federal University for the project part of the state assignment in the sphere of scientific activities and also supported by Russian Foundation for Basic Research (Grant 14-04-31029 mol_a).

References

Afonin S, Grage SL, Ieronimo M, Wadhwani P, Ulrich AS (2011) Temperaturedependent transmembrane insertion of the amphiphilic peptide PGLa in lipid bilayers observed by solid state 19F NMR spectroscopy. J Am Chem Soc 130:16512–16514. doi:10.1021/ja803156d

Arora A, Tamm LK (2001) Biophysical approaches to membrane protein structure determination. Curr Opin Struct Biol 11:540–547. doi:10.1016/S0959-440X(00)00246-3

Blochin DS et al (2013) Spatial structure of heptapeptide Glu-Ile-Leu-Asn-His-Met-Lys, a fragment of the HIV enhancer prostatic acid phosphatase, in aqueous and SDS micelle solutions. J Mol Struct 1033:59–66. doi:10.1016/j.molstruc.2012.08.018

Buffy JJ, Hong T, Yamaguchi S, Waring AJ, Lehrer RI, Hong M (2003) Solid-state NMR investigation of the depth of insertion of protegrin-1 in lipid bilayers using paramagnetic Mn2+. Biophys J 85:2363–2373. doi:10.1016/S0006-3495(03)74660-8

Chan DI, Prenner EJ, Vogel HJ (2006) Tryptophan- and arginine-rich antimicrobial peptides: structures and mechanisms of action. Biochim Biophys Acta 1758:1184–1202. doi:10.1016/j.bbamem.2006.04.006

Chen VB et al (2010) MolProbity: all-atom structure validation for macromolecular crystallography. Acta Crystallogr D 66:12–21. doi:10.1107/S0907444909042073

Choi MK et al (2014) Defining the genetic relationship of protegrin-related sequences and the in vivo expression of protegrins. FEBS J 281:5420–5431. doi:10.1111/Febs.13072

Cho Y, Turner JS, Dinh N-N, Lehrer RI (1998) Activity of protegrins against yeast-phase candida albicans. Infect Immun 66(6): 2486–2493

Davis IW et al (2007) MolProbity: all-atom contacts and structure validation for proteins and nucleic acids. Nucleic Acids Res 35:W375–W383. doi:10.1093/Nar/Gkm216

Delaglio F, Grzesiek S, Vuister GW, Zhu G, Pfeifer J, Bax A (1995) Nmrpipe—a multidimensional spectral processing system based on unix pipes. J Biomol NMR 6:277–293. doi:10.1007/Bf00197809

Elad S, Epstein JB, Raber-Durlacher J, Donnelly P, Strahilevitz J (2012) The antimicrobial effect of Iseganan HCl oral solution in patients receiving stomatotoxic chemotherapy: analysis from a multicenter, double-blind, placebo-controlled, randomized, phase III clinical trial. J Oral Pathol Med 41:229–234. doi:10.1111/j.1600-0714.2011.01094.x

Epand RF, Ramamoorthy A, Epand RM (2006) Membrane lipid composition and the interaction with Pardaxin: the role of cholesterol. Protein Pept Lett 13:1–5. doi:10.2174/092986651060201000 1

Fahrner RL, Dieckmann T, Harwig SSL, Lehrer RI, Eisenberg D, Feigon J (1996) Solution structure of protegrin-1, a broad-spectrum antimicrobial peptide from porcine leukocytes. Chem Biol 3:543–550. doi:10.1016/S1074-5521(96)90145-3

Galiullina LF, Blokhin DS, Aganov AV, Klochkov VV (2012) Investigation of cholesterol + model of biological membrane complex by NMR spectroscopy. Magn Reson Solids 14: 12204–12210

Gottler LM, La De, Salud-Bea R, Shelburne CE, Ramamoorthy A, Marsh ENG (2008) Using fluorous amino acids to probe the effects of changing hydrophobicity on the physical and biological properties of the -hairpin antimicrobial peptide protegrin-1. Biochemistry 47:9243–9250. doi:10.1021/bi801045n

Haney EF, Hunter HN, Matsuzaki K, Vogel HJ (2009) Solution NMR studies of amphibian antimicrobial peptides: linking structure to function? Biochim Biophys Acta 1788:1639–1655. doi:10.1016/j.bbamem.2009.01.002

Hiller S, Wagner G (2009) The role of solution NMR in the structure determinations of VDAC-1 and other membrane proteins. Curr Opin Struct Biol 19:396–401. doi:10.1016/j.sbi.2009.07.013

Hong M (2006) Solid-state NMR studies of the structure, dynamics, and assembly of beta-sheet membrane peptides and alpha-helical membrane proteins with antibiotic activities. Acc Chem Res 39:176–183. doi:10.1021/ar040037e

Hwang TL, Shaka AJ (1995) Water suppression that works—excitation sculpting using arbitrary wave-forms and pulsed-field gradients. J Magn Reson Ser A 112:275–279. doi:10.1006/jmra.1995.1047

Jang H, Ma B, Woolf TB, Nussinov R (2006) Interaction of protegrin-1 with lipid bilayers: membrane thinning effect. Biophys J 91:2848–2859. doi:10.1529/biophysj.106.084046

Jang H, Ma BY, Nussinov R (2007) Conformational study of the protegrin-I (PG-I) dimer interaction with lipid bilayers and its effect. BMC Struct Biol 7:21. doi:10.1186/1472-6807-7-21

Jang H, Ma B, Lal R, Nussinov R (2008) Models of toxic beta-sheet channels of protegrin-1 suggest a common subunit organization motif shared with toxic alzheimer beta-amyloid ion channels. Biophys J 95:4631–4642. doi:10.1529/biophysj.108.134551

Jenssen H, Hamill P, Hancock REW (2006) Peptide antimicrobial agents. Clin Microbiol Rev 19:491–511. doi:10.1128/Cmr.00056-05

Khayrutdinov BI, Bae WJ, Yun YM, Lee JH, Tsuyama T, Kim JJ, Hwang E, Ryu KS, Cheong HK, Cheong C, Ko JS, Enomoto T, Karplus PA, Güntert P, Tada S, Jeon YH, Cho Y (2009) Structure of the Cdt1 C-terminal domain: conservation of the winged helix fold in replication licensing factors. Protein Sci 18:2252–2264. doi:10.1002/pro.236

Kim K, Khayrutdinov BI, Lee CK, Cheong HK, Kang SW, Park H, Lee S, Kim YG, Jee JG, Rich, Kim KK, Jeon YH (2011) Solution structure of the Zβ domain of human DNA-dependent activator of IFN-regulatory factors and its binding modes to B-and Z-DNAs. Proc Natl Acad Sci USA 108:6921–6926. doi:10.1073/pnas.1014898107

Kokryakov VN et al (1993) Protegrins—leukocyte antimicrobial peptides that combine features of corticostatic defensins and tachyplesins. FEBS Lett 327:231–236. doi:10.1016/0014-5793(93)80175-T

Langham AA, Ahmad AS, Kaznessis YN (2008) On the nature of antimicrobial activity: a model for protegrin-1 pores. J Am Chem Soc 130:4338–4346. doi:10.1021/Ja0780380

Lazaridis T, He Y, Prieto L (2013) Membrane interactions and pore formation by the antimicrobial peptide protegrin. Biophys J 104:633–642. doi:10.1016/j.bpj.2012.12.038

Loury DJ, Embree JR, Steinberg DA, Sonis ST, Fiddes JC (1999) Effect of local application of the antimicrobial peptide IB-367 on the incidence and severity of oral mucositis in hamsters. Oral Surg Oral Med O 87:544–551. doi:10.1016/S1079-2104(99)70131-9

Mani R, Tang M, Wu X, Buffy JJ, Waring AJ, Sherman MA, Hong M (2006) Membrane-bound dimer structure of a beta-hairpin antimicrobial peptide from rotational-echo double-resonance solid-state NMR. Biochemistry 45:8341–8349. doi:10.1021/Bi060305b

Ovchinnikova TV, Shenkarev ZO, Balandin SV, Nadezhdin KD, Paramonov AS, Kokryakov VN, Arseniev AS (2008) Molecular insight into mechanism of antimicrobial action of the beta-hairpin peptide arenicin: specific oligomerization in detergent micelles. Biopolymers 89:455–464. doi:10.1002/bip.20865

Papo N, Shai Y (2004) Effect of drastic sequence alteration and D-amino acid incorporation on the membrane binding behavior of lytic peptides. Biochemistry 43:6393–6403. doi:10.1021/bi049944h

Pettersen EF, Goddard TD, Huang CC, Couch GS, Greenblatt DM, Meng EC, Ferrin TE (2004) UCSF chimera—a visualization system for exploratory research and analysis. J Comput Chem 25:1605–1612. doi:10.1002/Jcc.20084

Piotto M, Saudek V, Sklenar V (1992) Gradient-tailored excitation for single-quantum NMR-spectroscopy of aqueous-solutions. J Biomol NMR 2:661–665. doi:10.1007/Bf02192855

Porcelli F, Verardi R, Shi L, Henzler-Wildman KA, Ramamoorthy A, Veglia G (2008) NMR structure of the cathelicidin-derived human antimicrobial peptide LL-37 in dodecylphosphocholine micelles. Biochemistry 47:5565–5572. doi:10.1021/bi702036s

Powers JP, Tan A, Ramamoorthy A, Hancock RE (2005) Solution structure and interaction of the antimicrobial polyphemusins with lipid membranes. Biochemistry 44:15504–15513. doi:10.1021/bi051302m

Ramamoorthy A (2009) Beyond NMR spectra of antimicrobial peptides: dynamical images at atomic resolution and functional insights. Solid State Nucl Magn Reson 35:201–207. doi:10.1016/j.ssnmr.2009.03.003

Ramamoorthy A, Lee DK, Santos JS, Henzler-Wildman KA (2008) Nitrogen-14 solid-state NMR spectroscopy of aligned phospholipid bilayers to probe peptide–lipid interaction and oligomerization of membrane associated peptides. J Am Chem Soc 130:11023–11029. doi:10.1021/ja802210u

Roumestand C, Louis V, Aumelas A, Grassy G, Calas B, Chavanieu A (1998) Oligomerization of protegrin-1 in the presence of DPC micelles. A proton high-resolution NMR study. FEBS Lett 421:263–267. doi:10.1016/S0014-5793(97)01579-2

Saravanan R, Bhattacharjya S (2011) Oligomeric structure of a cathelicidin antimicrobial peptide in dodecylphosphocholine micelle determined by NMR spectroscopy. Biochim Biophys Acta 1808:369–381. doi:10.1016/j.bbamem.2010.10.001

Schwieters CD, Kuszewski JJ, Tjandra N, Clore GM (2003) The Xplor-NIH NMR molecular structure determination package. J Magn Reson 160:65–73. doi:10.1016/S1090-7807(02)00014-9

Shai Y (2002) From innate immunity to de-novo designed antimicrobial peptides. Curr Pharm Des 8:715–725. doi:10.2174/1381612023395367

Sklenar V, Piotto M, Leppik R, Saudek V (1993) Gradient-tailored water suppression for H-1-N-15 HSQC experiments optimized to retain full sensitivity. J Magn Reson Ser A 102:241–245. doi:10.1006/jmra.1993.1098

Syvitski RT, Burton I, Mattatall NR, Douglas SE, Jakeman DL (2005) Structural characterization of the antimicrobial peptide pleurocidin from winter flounder. Biochemistry 44:7282–7293. doi:10.1021/bi0504005

Trotti A et al (2004) A multinational, randomized phase III trial of iseganan HCL oral solution for reducing the severity of oral mucositis in patients receiving radiotherapy for head-and-neck malignancy. Int J Radiat Oncol 58:674–681. doi:10.1016/S0630-3016(04)01627-4

Usachev KS, Filippov AV, Antzutkin ON, Klochkov VV (2013) Use of a combination of the RDC method and NOESY NMR spectroscopy to determine the structure of Alzheimer's amyloid A beta(10-35) peptide in solution and in SDS micelles. Eur Biophys J Biophy 42:803–810. doi:10.1007/s00249-013-0928-7

Usachev KS, Efimov SV, Kolosova OA, Filippov AV, Klochkov VV (2014a) High-resolution NMR structure of the antimicrobial peptide protegrin-2 in the presence of DPC micelles. J Biomol NMR (in press). doi:10.1007/s10858-014-9885-4

Usachev KS, Filippov AV, Khairutdinov BI, Antzutkin ON, Klochkov VV (2014b) NMR structure of the Arctic mutation of the Alzheimer's A beta(1-40) peptide docked to SDS micelles. J Mol Struct 1076:518–523. doi:10.1016/j.molstruc.2014.08.030

Vivcharuk V, Kaznessis YN (2010) Dimerization of protegrin-1 in different environments. Int J Mol Sci 11:3177–3194. doi:10.3390/Ijms11093177

Wang G (2007) Determination of solution structure and lipid micelle location of an engineered membrane peptide by using one NMR experiment and one sample. Biochim Biophys Acta 1768:3271–3281. doi:10.1016/j.bbamem.2007.08.005

Yamaguchi S, Hong T, Waring A, Lehrer RI, Hong M (2002) Solid-state NMR investigations of peptide-lipid interaction and orientation of a ss-sheet antimicrobial peptide, protegrin. Biochemistry-US 41:9852–9862. doi:10.1021/Bi0257991

Zamoon J, Nitu F, Karim C, Thomas DD, Veglia G (2005) Mapping the interaction surface of a membrane protein: unveiling the conformational switch of phospholamban in calcium pump regulation. Proc Natl Acad Sci USA 102:4747–4752. doi:10.1073/pnas.0406039102

Zanetti M, Gennaro R, Romeo D (1995) Cathelicidins: a novel protein family with a common proregion and a variable C-terminal antimicrobial domain. FEBS Lett 374:1–5. doi:10.1016/0014-5793(95)01050-O

Zhao CQ, Liu LD, Lehrer RI (1994) Identification of a new member of the protegrin family by cdna cloning. FEBS Lett 346:285–288. doi:10.1016/0014-5793(94)00493-5

Zhao CQ, Ganz T, Lehrer RI (1995) The structure of porcine protegrin genes. FEBS Lett 368:197–202. doi:10.1016/0014-5793(95)00633-K